Environmental and Climate Technologies
2025, vol. 29, no. 1, pp. 433–446
https://doi.org/10.2478/rtuect-2025-0029
https://content.sciendo.com

Techno-Economic Optimization of Solar Panel Installations: Balancing Thermal Performance and Economic Viability

Kudzanayi CHITEKA[1]*, Christopher ENWEREMADU[2]

[1,2]*Department of Mechanical Engineering, University of South Africa, Science Campus, Florida 1710, South Africa*

Received 13.03.2025; accepted 16.06.2025

***Abstract* – As solar energy gains prominence, optimizing panel configurations for efficiency and cost-effectiveness is crucial. This study examines the impact of installation height and tilt angle on thermal performance, power output, and structural constraints. Using computational models, the study optimized height and tilt to enhance cooling and minimize costs. Increased heights improved air circulation, reducing cell temperatures and boosting efficiency through passive cooling. Higher tilt angles enhanced heat dissipation via air turbulence but also raised wind loading, necessitating stronger, costlier support structures. The optimal configuration of 0.165 meters height and 25.022° tilt balanced efficiency and structural demands. This setup achieved a Levelized Cost of Energy (LCoE) of $ 0.07/kWh, an ROI of 16.3 %, and a payback period of 6.25 years. Compared to a non-optimized setup (7.5 meters height, 75° tilt), this reduced LCoE by 42 %, improved ROI by 60 %, and shortened the payback period by 37.5 %. The findings highlight the importance of tailored height and tilt to maximize efficiency while controlling costs. Future research should explore different installation surfaces and climate conditions to further refine the balance between performance and cost.**

***Keywords* – Economic viability; elevated installations; installation optimization; structural integrity; techno-economic analysis; thermal performance.**

Nomenclature		
H_p	Solar panel height	m
$k-\epsilon$	k– epsilon Turbulence Model	–
P_κ	Turbulent kinetic energy production	W/m^3
R^2	Coefficient of determination	–
(SST) $k-\omega$	Shear Stress Transport k–omega Turbulence Model	–
T_{ref}	Reference temperature	°C
η_{ref}	Reference efficiency	%
$\bar{p}$	Time-averaged Pressure	Pa
$\bar{u}$	Time-averaged Velocity	m/s
$\bar{\rho}$	Time-averaged Density	kg/m^3/s
α	Temperature coefficient of power	°C^{-1}

* Corresponding author.
E-mail address: echitekk@unisa.ac.za

β and β*	Model constants	–
η(*T*)	Efficiency at operating temperature *T*	%
κ	Turbulent Kinetic Energy	m^2/s^2
μ	Dynamic Viscosity	$N\cdot s/m^2$
σ_κ	Turbulent Prandtl number for κ	–
σ_ω	Turbulent Prandtl number for ω	–
τ	Reynolds Stresses	Pa
ω	Specific Dissipation Rate	s^{-1}

1. INTRODUCTION

The transition to renewable energy is vital for meeting global energy demands and combating climate change. Solar energy, due to its abundance and sustainability, has become a cost-competitive alternative, with Levelized Cost of Energy (LCoE) ranging from $ 0.04/kWh to $ 0.14/kWh, often cheaper than coal power [1], [2]. Its versatility has led to widespread applications, including integration into sustainable building designs and energy-efficient infrastructure [3]–[5]. Solar panel performance depends on irradiance, temperature, soiling, and installation geometry. Dust and shading can reduce power by up to 58 % [6] while high temperatures lower efficiency, necessitating cooling mechanisms for optimal performance [7].

Rising temperatures increase electron-hole recombination, reducing open-circuit voltage and fill factor, ultimately lowering efficiency [8]. Studies show that higher PV module temperatures decrease output power and voltage [9]. This is due to the temperature coefficient, which for silicon cells is −0.4 % to −0.5 % per °C above 25 °C, leading to power loss [10]. Elevated temperatures also alter band gaps and shorten panel lifespan [11]. Mounting panels higher improves cooling through enhanced convection, with double-height panels achieving 1.88 times better heat dissipation [12], [13]. Smith *et al*. [13] found that increased height lowers surface temperatures by 4.4 °C, boosting energy output by 0.5 %–2.25 %. Greater height also increases wind speed, improving cooling but potentially introducing mechanical stress [14].

Installation geometry critically affects solar PV performance, with tilt and azimuth angles influencing solar radiation absorption, heat dissipation, and efficiency. Optimal tilt maximizes energy capture while aiding heat dissipation, whereas deviations increase heat build-up and reduce efficiency [15]. Studies show that moderate deviations in West and Central Africa cause <5 % irradiation loss [16], while in India, seasonal tilt adjustments increase radiation absorption by 2.41 % and capacity utilization by 0.26 % [17].

Solar cell performance is heavily influenced by material choice, particularly regarding temperature variations. Silicon-based cells lose efficiency as temperatures rise due to increased electron-hole recombination, with mono-crystalline silicon performing better in cooler conditions [18], [19]. Polycrystalline silicon (pc-Si) exhibits lower power loss at high temperatures, while thin-film technologies like Cadmium Telluride (CdTe) and Copper Indium Gallium Diselenide (CIGS) Solar Cells maintain better efficiency due to lower temperature sensitivity [8], [18]. Amorphous modules operate at higher temperatures, affecting efficiency, while crystalline silicon degrades more slowly, ensuring better long-term performance [20].

To mitigate temperature-induced losses, solar PV systems utilize passive and active cooling methods, including water, air, phase-change materials, and advanced techniques like geothermal and jet impingement cooling [21], [22]. Cooling can lower panel temperatures by up to 49.2 °C and boost efficiency by 47.67 % [21]. Innovations like Photovoltaic Thermal (PV/T) hybrids, microtechnology-based cooling, and passive radiative or evaporative cooling show promise, requiring careful design for optimal performance [22], [23].

Wind loading impacts the design of solar arrays, affecting structural integrity and performance. Wind direction, array configuration, and panel tilt influence lift and drag forces. In floating PV systems, the first and last rows experience the highest forces, while middle rows benefit from a sheltering effect, reducing wind impact by 45–86 % [24]. Tracking systems, especially single-axis and dual-axis, optimize solar exposure, increasing power generation by 24.4 % and 32.2 %, respectively, compared to fixed systems [25]. However, their high installation and maintenance costs can reduce economic viability. Advancements in adaptive tracking algorithms can improve efficiency while lowering operational costs [26]. Choosing the right support structure is essential for balancing performance and cost. Techno-economic optimization of solar panels is key to maximizing efficiency and minimizing costs. Kolhe [27] presented a method to optimize stand-alone PV systems, focusing on the relationship between PV array and battery capacity. Kumar *et al.* [28] found that annual optimum tilt with fixed installations was most suitable for rural healthcare buildings. These studies used tools like levelized cost of energy, HOMER software, and Monte Carlo methods to identify optimal configurations.

Installing solar panels at higher elevations improves wind flow, cooling the panels and enhancing their efficiency [29]. Elevated temperatures can reduce panel performance, but increasing tilt angles allows for greater solar irradiance and higher energy output. However, this must be balanced against thermal losses due to higher temperatures. Glick *et al*. [30] found that turbulence increases convective heat transfer by 7 %, and panel angles up to 30° enhance convection. Reynolds shear stress and buoyancy further improve mixing and heat dissipation.

While previous studies have addressed individual aspects of solar PV performance, such as thermal losses, structural design, or cost analysis, few have offered a unified optimization framework that simultaneously considers thermal performance, structural integrity, and economic viability. This study uniquely integrates Computational Fluid Dynamics (CFD), Finite Element Analysis (FEA), and economic modelling to determine optimal panel installation configurations. Unlike prior work that often isolates thermal or structural factors, the present approach quantifies the trade-offs between enhanced cooling, wind-induced structural loading, and associated costs. The novelty lies not only in this comprehensive, simulation-based methodology but also in the inclusion of a field experiment that validates the structural simulations under real atmospheric conditions. By comparing experimental stress measurements with numerical predictions, the study confirms the suitability of the models used and enhances their real-world relevance. Furthermore, the study's focus on tailoring installations to site-specific climate and wind profiles provides actionable insights for practical deployment in similar regions, bridging a gap between theoretical analysis and empirical application. The rest of this manuscript is structured as follows: Section 2 will outline the methodological approach, Section 3 will present the results and discussions, followed by conclusions and recommendations in Section 4.

2. METHODOLOGY

This study adopts a multidisciplinary approach to analyse the techno-economic performance of solar panel installations, focusing on thermal, economic, and structural aspects. It integrates Computational Fluid Dynamics (CFD) simulations to assess wind loads and Finite Element Analysis (FEA) using ANSYS Mechanical to evaluate structural integrity. CFD models airflow and FEA models the stresses on support structures to ensure durability under environmental conditions.

The study site, Roodepoort, South Africa (26.1590° S, 27.8619° E), was selected for its diverse climate and strong solar energy potential, receiving 4.9–7.6 kWh/m²/day of solar insolation. With average wind speeds of 3.5 m/s aiding panel cooling, ambient temperatures ranging from 10 °C to 28 °C, and 60 % relative humidity, the location provides ideal conditions for analysing installation height, tilt angles, and performance.

The study systematically varied panel installation heights from 0.5 m to 5.5 m to assess cooling effects and thermal dynamics. Tilt angles ranged from 15° to 75° to optimize solar irradiance capture. By testing multiple height and tilt configurations, the study quantified their impact on the thermal and structural performance of the solar array. Surface temperatures were monitored to evaluate how these parameters mitigate heat build-up and enhance efficiency. The analysis also examined airflow effectiveness in cooling panels and its correlation with energy output. Jinko 550 W monocrystalline panels were used, with specifications detailed in Table 1.

TABLE 1. SPECIFICATIONS OF JINKO 550W MONOCRYSTALLINE PHOTOVOLTAIC PANEL

Specification	**Value**
Model	Jinko 550 W
Type	Monocrystalline
Dimensions	2278 × 1134 × 35 mm
P_{max}	550 W
η_{max}	20.64 %
V_{mp}	48.0 V
I_{mp}	11.46 A
V_{oc}	58.0 V
I_{sc}	12.12 A
β	−0.35 %/°C
Operating Temperature Range	−40 °C to +85 °C

2.1. Wind Flow Analysis

The CFD approach in this study used the Reynolds-Averaged Navier-Stokes (RANS) Eqs. (1–2), combined with the Shear Stress Transport (SST) k−ω turbulence model Eqs. (3–4). The (SST) k−ω turbulence model was chosen for its ability to predict flow separation and pressure distribution, especially in adverse pressure gradients. It combines the k−ω model's strengths in near-wall regions with the k−ϵ model's strengths in free-stream regions [31], making it suitable for simulating complex flows around solar panels under varying wind conditions. The RANS equations describe the time-averaged flow field, essential for modelling turbulent flows in real-world scenarios, where $\bar{\rho}$ is time-averaged density, $\bar{u}$ is time-averaged velocity, and $\bar{p}$ is time-averaged pressure, with μ as dynamic viscosity and τ representing Reynolds stresses.

$$\frac{\partial \bar{\rho}}{\partial t} + \nabla \cdot (\bar{\rho}\bar{u}) = 0, \tag{1}$$

$$\frac{\partial}{\partial t}(\bar{\rho}\bar{u}) + \nabla \cdot (\bar{\rho}\bar{u}\bar{u}) = -\nabla \cdot \bar{p} + \nabla \cdot (\mu \nabla \bar{u}) + \bar{\rho} g + \nabla \cdot \tau, \tag{2}$$

$$\frac{\partial(\rho k)}{\partial t} + \nabla \cdot (\rho k u) = \nabla \cdot \left(\frac{\mu_t}{\sigma_\omega} \nabla k \right) + P_k - \beta^* \rho \omega, \tag{3}$$

$$\frac{\partial(\rho \omega)}{\partial t} + \nabla \cdot (\rho \omega u) = \nabla \cdot \left(\frac{\mu_t}{\sigma_\omega} \nabla \omega \right) + \frac{\beta \omega}{k} P_k - \rho \omega^2, \tag{4}$$

where P_κ is the production of turbulent kinetic energy, β and β^* are model constants, σ_κ is the turbulent Prandtl number for κ while σ_ω is the turbulent Prandtl number for ω.

In this study, the computational domain was developed to model flow dynamics around the solar panel array, enabling effective analysis of wind loading and thermal performance. The 3D domain shown in Fig. 1 (where H_p is the solar panel height) was developed to replicate the atmospheric boundary layer. A structured mesh was used in the far-field region for accuracy and efficiency, as it enhances performance in simpler geometries [32], [33]. A hybrid meshing approach combining unstructured meshes around the solar panels with structured meshes in the far-field was used, reducing complexity and optimizing computation through multi-blocking and load balancing [34], [35].

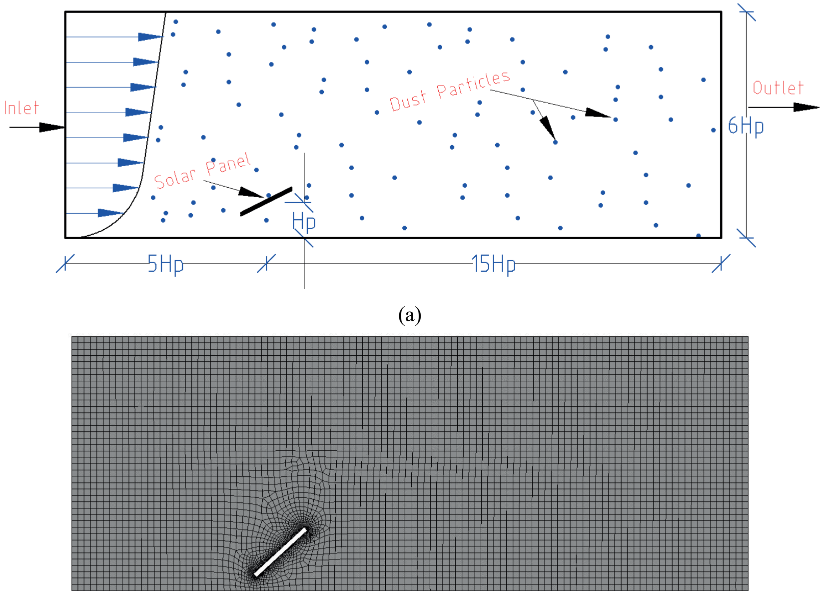

(a)

(b)

Fig. 1. (a) Computational domain configuration representing wind flow around the solar panel array, and (b) the structural mesh used in the study highlighting a fine mesh close to the solar panel.

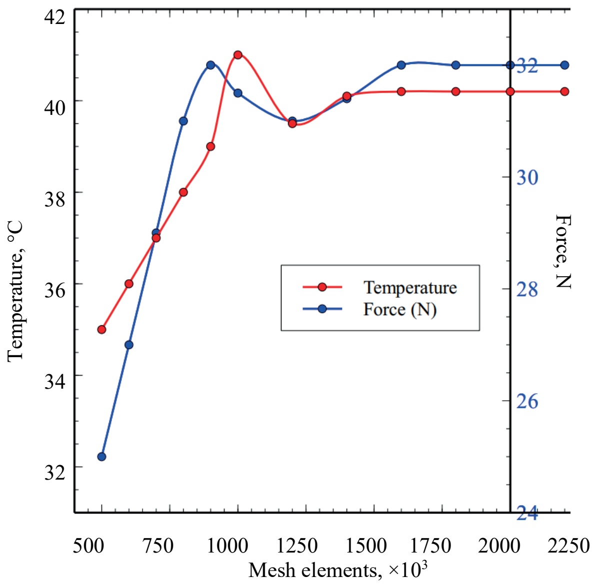

Fig. 2. Grid Independence Analysis showing the variation in Key Performance Indicators across different mesh sizes.

A grid independence analysis (shown in Fig. 2) was performed with coarse (750 000 elements), medium (1.5 million), and fine (2.25 million) meshes. The medium mesh balanced accuracy and efficiency, with minimal differences (<5 %) from the fine mesh, confirming solution convergence.

Boundary conditions simulated wind flow and thermal interactions around the solar panel array. Inlet wind velocity profiles were based on Roodepoort's atmospheric boundary layer data, with a pressure outlet and symmetry on the side walls. A User Defined Function (UDF) accounted for wind speed and temperature variations. The study considered drag and Saffman lift forces, and thermophoretic effects. Convergence was ensured by reducing residuals below 1×10^{-5} for key variables. The solar panel was modelled as a wall with a no-slip condition. Airflow at the inlet was controlled via a UDF, based on NASA data [36].

2.2. Validation of CFD Simulations

To validate the CFD simulations, the velocity profiles and turbulent kinetic energy (TKE) profiles were compared with experimental data from wind tunnel experiments by Tomilaga *et al*. [37] (see Fig. 3), which serve as reliable benchmarks for modelling wind flow around solar panel arrays. The results showed a deviation of 2.37 %, indicating strong agreement between the simulations and experimental data.

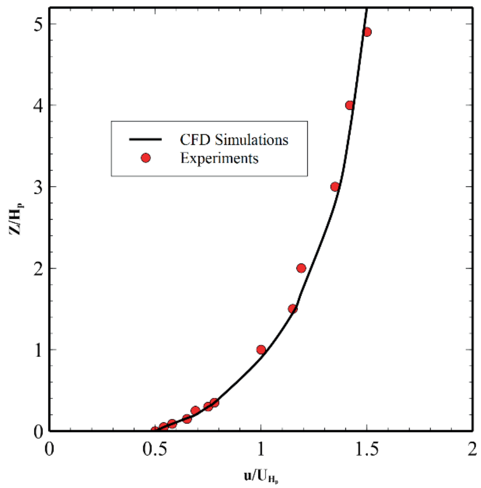

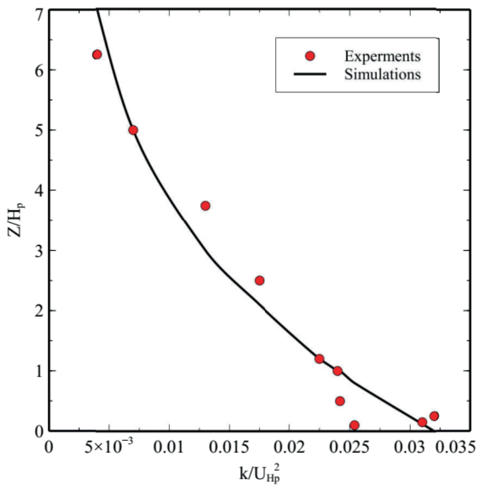

Fig. 3. Comparison of inlet profiles between CFD Simulations and Wind Tunnel Experiments by Tomilaga *et al.* [36]: (a) mean fluid air velocity $\left(\frac{u}{U_{H_p}}\right)$, and (b) turbulent kinetic energy $\left(\frac{k}{U_{H_p}^2}\right)$.

2.3. Structural and Thermal Analysis

In addition to the CFD analysis, a structural mesh for Finite Element Analysis of the support structures was developed as seen in Fig. 4. A tetrahedral mesh was used for flexibility in modelling complex geometries and accurately capturing stress distributions. The element size was 5 mm around critical stress points, with approximately 800 000 elements. Structural steel was selected with a yield strength of 250 MPa and ultimate tensile strength of 450 MPa.

The support structure was modelled as a cantilever beam anchored to the ground, with forces from the CFD simulations applied at the top. These forces were integrated into the ANSYS mechanical model to simulate wind loading at different heights and tilt angles of the solar panels. Boundary conditions included a fixed support at the base and wind loads at the top. The structural analysis focused on stress distribution and deformation under wind loading, identifying critical failure points and assessing stability to determine the minimum allowable dimensions of a cylindrical structural steel tube for each scenario.

A field experiment was conducted using a 20 W monocrystalline solar panel mounted on a steel pillar-type support structure at the University of South Africa’s Florida campus to enhance the real-world applicability of the simulation findings. This experimental setup replicated the structural parameters used in the finite element model, including material properties. The panel was installed at a fixed height of 3 m with a 30° tilt to simulate typical small-scale deployment. High-precision foil-type strain gauges were affixed at critical stress zones along the support, particularly near the base and mid-height, to capture stress responses under ambient wind conditions. Strain data were continuously logged using a data acquisition system over several days, with concurrent wind speed measurements recorded via an anemometer. The recorded strain was converted into stress using standard relationships and compared with ANSYS Mechanical simulation outputs. The experiment validated the numerical models by confirming stress trends and structural responses, while also revealing transient fluctuations and localized effects.

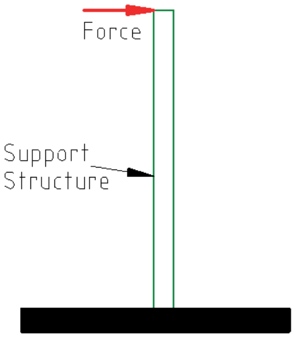

Fig. 4. Structural representation of support structures for Finite Element Analysis.

The thermal performance assessment evaluated the impact of wind cooling on solar panel efficiency and power generation. It integrated CFD simulation data with temperature-power conversion models to estimate panel operating temperatures under varying conditions, considering factors like wind speed, panel height, tilt angle, and ambient temperature. Eq. (5) was used to define the efficiency and, by extension, the power and energy generated at various temperatures. The efficiency at operating temperature T is represented by $\eta(T)$, the reference efficiency by η_{ref}, the temperature coefficient by α, and the reference temperature by T_{ref}.

$$\eta(T) = \eta_{ref}\left[1 - \alpha\left(T - T_{ref}\right)\right] \tag{5}$$

2.4. Economic Analysis and Optimization

The economic evaluation assessed whether the power gains from improved thermal performance at higher solar panel installations justify the additional costs of support structures, installation, and maintenance. Financial metrics like payback period, Levelized Cost of Energy (LCoE), and return on investment (ROI) were used, factoring in cooling effects that enhance efficiency and energy generation at elevated heights.

The optimization process aimed to identify the most cost-effective configuration of support structures by balancing structural integrity with material cost, ensuring the structure could withstand wind-induced forces while minimizing material usage and keeping stress below the yield strength of structural steel. Additionally, the process focused on maximizing the net benefit of each installation height, balancing total costs (structural, installation, and maintenance) with gains in energy production, to identify the optimal installation height.

3. Results and Discussions

3.1. Thermal Performance Analysis

The study found that increasing the installation height of solar panels leads to lower temperatures due to improved air circulation and wind exposure, enhancing thermal performance and efficiency, with a coefficient of determination (R^2) of 0.64. Additionally, turbulent kinetic energy profiles, see Fig. 5, revealed that higher installation heights result in more pronounced TKE, boosting convective cooling, reducing panel temperatures, and improving efficiency.

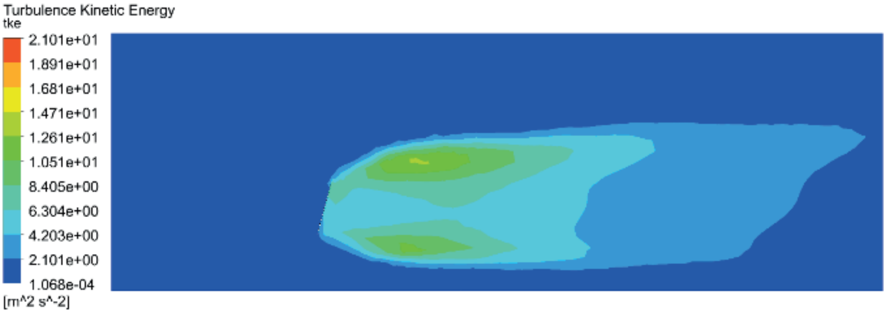

(a)

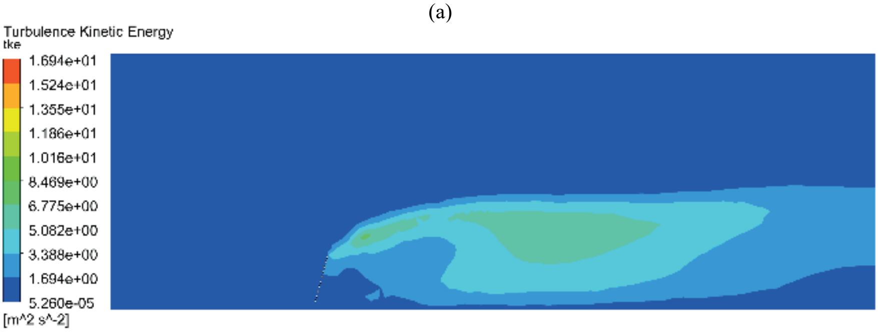

(b)

Fig. 5. The impact of height on temperature as illustrated in turbulent kinetic energy profiles at 75° tilt at installation heights of: (a) 5.5 m and (b) 0.5 m.

Elevated solar panel installations reduce thermal losses by maintaining lower temperatures, improving efficiency through increased TKE and enhanced heat dissipation. Higher tilt angles (75°) create more turbulence around the panels, improving convective cooling and reducing temperatures, whereas lower tilt angles (15°) lead to laminar airflow, limiting heat dissipation and potentially lowering efficiency. Elevated installation heights and lower tilt angles generally reduce solar cell temperatures as opposed to higher tilt angles and lower heights. Elevated setups with moderate tilt angles benefit from improved cooling, but higher tilt angles lead to higher temperatures due to increased solar radiation exposure. This highlights the importance of balancing tilt angle and height for optimal temperature management.

The cooling benefits from increased installation height and proper tilt angles result in improved panel efficiency, with a maximum efficiency gain of 1.72 % observed at a height of 5.5 m. Although only 20.64 % of solar irradiance is converted to electricity, effective temperature management, particularly through tilt angles, can minimize thermal losses. However, in low-wind conditions, higher tilt angles may increase heat accumulation, reducing efficiency.

3.2. Structural Integrity

In this study, the stress distribution and deformation of solar panel support structures under varying wind loads were analysed using Finite Element Analysis (FEA), highlighting the influence of installation height and tilt angle on structural response. The support structures, modelled as hollow cylindrical steel tubes with a yield strength of 250 MPa, exhibited a strong dependence on height, as shown in Fig. 6. The simulations revealed that higher elevations subjected the panels to increased wind forces, necessitating stronger and more resilient support systems. Additionally, higher tilt angles increased the surface area exposed to wind loading, further amplifying structural demands. While these angles can enhance energy capture, they introduce a trade-off with mechanical stability and material cost, emphasizing the need for optimized design.

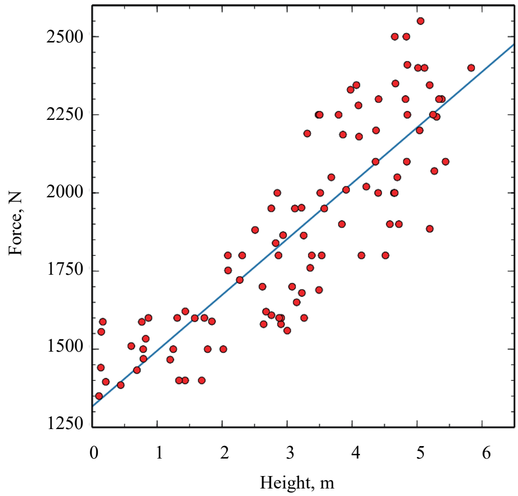

Fig. 6. A scatter plot showing the relationship between height and forces induced by increased wind loading as the height increased from 0.5 m to 5.5 m.

The experimental results from the field experiment closely mirrored the simulated stress distributions, particularly showing peak stress near the base of the support, consistent with cantilever beam behaviour. The average percentage difference between experimental and simulated stress values was 6.8 %. Furthermore, transient wind-induced fluctuations observed in the experiment echoed the variations predicted by CFD-based load profiles.

3.3. Economic Evaluation and Optimisation

The analysis of the relationship between height and structural costs, as well as height and revenue, highlights the complexity of optimizing solar panel installations for both economic and thermal performance. The study shows that increasing installation height improves power generation due to cooler temperatures, enhancing panel efficiency. The maximum revenue of $ 23 934.92 was observed at a height of 5.06 m and a tilt of 69.54°, resulting in a cell temperature of 61.34 °C and an efficiency of 18 %. In contrast, the maximum structural cost of $ 32 084.15 occurred at a height of 5.834 m and a tilt of 73.42°, resulting in a cell temperature of 54.32 °C and an efficiency of 18.5 %. Fig. 7 illustrates the trade-offs: while higher heights can increase revenue through enhanced energy output, they also lead to higher initial costs due to stronger materials and more complex installations. These findings underscore the need for a careful cost-benefit analysis to find an optimal balance between thermal performance, power generation, and structural costs.

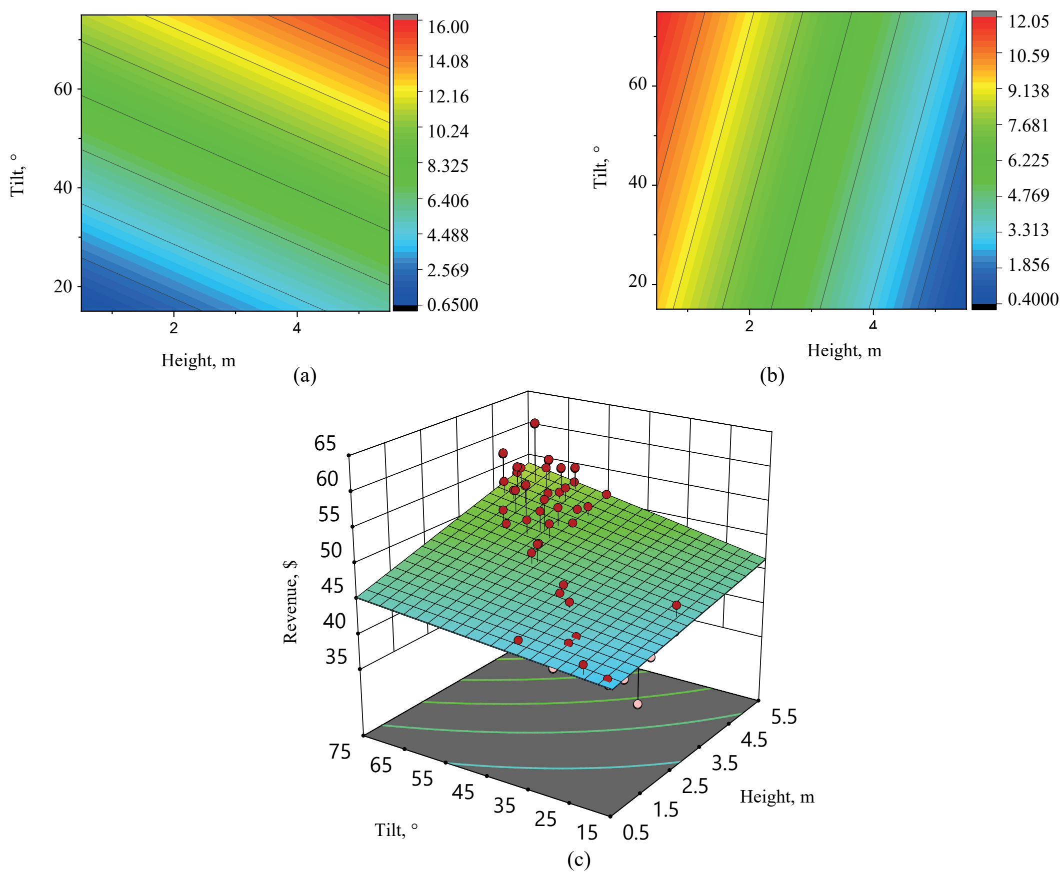

Fig. 7. The contours illustrate the relationships between: (a) tilt, height, and cost; (b) tilt, height, and revenue; and (c) the response surface depicting the effects of tilt and height on generated revenues. All values are in USD (×10^3).

The study examined the relationship between installation height, tilt angle, and both costs and revenues, with findings highlighted in Fig. 8. As depicted in Fig. 8(a), increased installation height generally reduces cell temperature and improves efficiency, this benefit is offset by higher wind loading at greater heights, which leads to greater heat loss through forced convection. As a result, the height does not show a clear correlation with revenue, and installations higher than 2.5 meters lead to increased structural costs, making revenues lower than costs. Fig. 8(b) illustrates that as tilt angles increase, revenue decreases due to higher solar cell temperatures and stronger wind forces, both of which necessitate more robust and costly structures. Up to a 35° tilt, revenue remains higher than costs, but beyond this point, the costs outweigh the revenue.

The study found that moderate installation height and tilt provide the best balance between energy yield and cost. The optimal configuration, with a height of 0.165 meters and a tilt of 25.022°, maximized revenue at $ 11 731.56 with a cost of $ 2107.52 over 25 years. This configuration achieved an LCoE of $ 0.07/kWh, significantly lower than the non-optimized setup with a height of 7.5 meters and a tilt of 75°, which had an LCoE of $ 0.12/kWh. The optimized configuration also resulted in a higher ROI of 16.3 % and a shorter payback period of 6.25 years, compared to the non-optimized configuration with an ROI of 10.18 % and a payback period of 10.3 years. These findings demonstrate the economic advantages of careful optimization of height and tilt for solar installations, offering a 60 % improvement in ROI and a 37.51 % reduction in payback period.

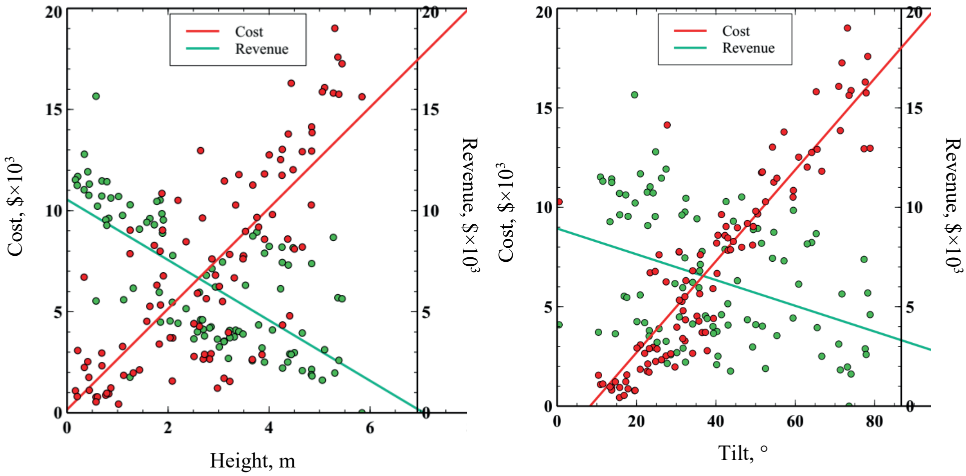

(a) (b)

Fig. 8. Optimisation of the installation height and tilt in relation to the costs and revenues.

4. Conclusions, Recommendations and Areas for Further Study

This study explored the effects of installation height and tilt angle on the thermal performance, structural integrity, and economic viability of solar panel installations. The findings showed that increasing the installation height improved thermal performance by reducing panel temperatures due to enhanced air circulation, which, in turn, boosted panel efficiency. However, this benefit was counterbalanced by the increased structural costs associated with elevated installations, which were exposed to stronger wind forces. The study found that while maximum efficiency gains occurred at a height of 5.5 meters, the trade-off between structural costs and efficiency gains should be considered when designing solar installations.

Economically, the study identified an optimal configuration with a height of 0.165 meters and a tilt angle of 25.022°. This configuration resulted in a competitive Levelized Cost of Energy (LCoE) of $ 0.07/kWh, with a significant ROI of 16.3 % and a reduced payback period of 6.25 years. In comparison, a non-optimized configuration with a height of 7.5 meters and a tilt of 75° had a higher LCoE of $ 0.12/kWh, a lower ROI, and a longer payback period. The findings highlighted the importance of balancing height and tilt to achieve both efficient energy production and cost-effectiveness.

The study also made several recommendations, including the adoption of the optimized configuration for maximum energy production while controlling costs, conducting thorough cost-benefit analyses before initiating solar projects, and investing in high-strength materials and innovative construction techniques to minimize structural costs. Additionally, future research should focus on the impact of surface roughness on airflow and thermal dynamics, the performance of solar installations in diverse climates, and the integration of active cooling systems to further improve thermal management.

REFERENCES

[1] Junedi M. M., Ludin N. A., Hamid N. H., Kathleen P. R., Hasila J., Ahmad Affandi N. A. Environmental and economic performance assessment of integrated conventional solar photovoltaic and agrophotovoltaic systems. *Renewable and Sustainable Energy Reviews* 2022:168:112799. https://doi.org/10.1016/j.rser.2022.112799
[2] Breyer C. Low-cost solar power enables a sustainable energy industry system. *Proceedings of the National Academy of Sciences* 2021:118(49):e2116940118. https://doi.org/10.1073/pnas.2116940118
[3] Albatayneh A., Albadaineh R. Evaluating Shading Effects of PV Systems: Discrepancies in Simulation Software and Energy Consumption. *Environmental and Climate Technologies* 2023:27(1):407–421. https://doi.org/10.2478/rtuect-2023-0030
[4] Grinevičiūtė M., Valančius K. Virtual Prosumers and the Impact of Remote Solar Parks on Lithuania's Buildings Decarbonization Efforts. *Environmental and Climate Technologies* 2024:28(1):312–328. https://doi.org/10.2478/rtuect-2024-0025
[5] Valdmanis G., Rieksta M., Luksta I., Bazbauers G. Solar Energy Based Charging for Electric Vehicles at Fuel Stations. *Environmental and Climate Technologies* 2022:26(1):1169–1191. https://doi.org/10.2478/rtuect-2022-0088
[6] Hasan D. S., Farhan M. S., ALRikabi H. TH. S. The effect of irradiance, tilt angle, and partial shading on PV performance. *AIP Conference Proceedings* 2023:2457(1):050008. https://doi.org/10.1063/5.0120692
[7] Khanafer K., Al-Masri A., Marafie A., Vafai K. Thermal performance of solar photovoltaic panel in hot climatic regions: Applicability and optimization analysis of PCM materials. *Numerical Heat Transfer, Part A: Applications* 2024:85(10):1612–1632. https://doi.org/10.1080/10407782.2023.2207732
[8] Shaker L. M., Al-Amiery A. A., Hanoon M. M., Al-Azzawi W. K., Kadhum A. A. H. Examining the influence of thermal effects on solar cells: a comprehensive review. *Sustainable Energy Research* 2024:11(1):6. https://doi.org/10.1186/s40807-024-00100-8
[9] Mohammad A. T., Al-Shohani W. A. M. Numerical and experimental investigation for analyzing the temperature influence on the performance of photovoltaic module. *AIMS Energy* 2022:10(5):1026–1045. https://doi.org/10.3934/energy.2022047
[10] Green M. A., Emery K., Hishikawa Y., Warta W. Solar Cell Efficiency Tables (Version 35). *Progress in Photovoltaics: Research and Applications* 2010:18(2):144–150. https://doi.org/10.1002/pip.974
[11] Dhass A. D., Natarajan E., Lakshmi P. An investigation of temperature effects on solar photovoltaic cells and modules. *International Journal of Engineering, Transactions B: Applications* 2014:27(11):1713–1722. https://doi.org/10.5829/idosi.ije.2014.27.11b.09
[12] Williams H. J., Hashad K., Wang H., Zhang K. M. The potential for agrivoltaics to enhance solar farm cooling. *Applied Energy* 2023:332:120478. https://doi.org/10.1016/j.apenergy.2022.120478
[13] Smith S. E., Viggiano B., Ali N., Silverman T. J., Obligado M., Calaf M., Cal R. B. Increased panel height enhances cooling for photovoltaic solar farms. *Applied Energy* 2022:325:119819. https://doi.org/10.1016/j.apenergy.2022.119819
[14] Osma G., Ordóñez G., Hernández E., Quintero L., Torres M. The impact of height installation on the performance of PV panels integrated into a green roof in tropical conditions. *WIT Transactions on Ecology and the Environment* 2016:205:147–156. https://doi.org/10.2495/EQ160141
[15] Mamun M. A. A., Islam M. M., Hasanuzzaman M., Selvaraj J. Effect of tilt angle on the performance and electrical parameters of a PV module: Comparative indoor and outdoor experimental investigation. *Energy and Built Environment* 2022:3(3):278–290. https://doi.org/10.1016/j.enbenv.2021.02.001
[16] N'Tsoukpoe K. E. Effect of orientation and tilt angles of solar collectors on their performance: Analysis of the relevance of general recommendations in the West and Central African context. *Scientific African* 2022:15:e01069. https://doi.org/10.1016/j.sciaf.2021.e01069
[17] Sharma G. S., Mahela O. P., Hussien M. G., Khan B., Padmanaban S., Shafik M. B., Elbarbary Z. M. S. Performance Evaluation of a MW-Size Grid-Connected Solar Photovoltaic Plant Considering the Impact of Tilt Angle. *Sustainability* 2022:14(3):1444. https://doi.org/10.3390/su14031444
[18] Dubey S., Sarvaiya J. N., Seshadri B. Temperature Dependent Photovoltaic (PV) Efficiency and Its Effect on PV Production in the World – A Review. *Energy Procedia* 2013:33:311–321. https://doi.org/10.1016/j.egypro.2013.05.072
[19] Ur Rehman S., Farooq M., Qamar A., Usman M., Ahmad G., Sultan M., Saleem M. W., Hussain I., Imran M., Ali Q., Javaid M. Y., Siddiqui F. A. Experimental investigation to thermal performance of different photo voltaic modules for efficient system design. *Alexandria Engineering Journal* 2022:61(12):12623–12634. https://doi.org/10.1016/j.aej.2022.06.037
[20] Adeeb J., Farhan A., Al-Salaymeh A. Temperature Effect on Performance of Different Solar Cell Technologies. *Journal of Ecological Engineering* 2019:20(5):249–254. https://doi.org/10.12911/22998993/105543
[21] Bilen K., Erdoğan İ. Effects of cooling on performance of photovoltaic/thermal (PV/T) solar panels: A comprehensive review. *Solar Energy* 2023:262:111829. https://doi.org/10.1016/j.solener.2023.111829
[22] Satpute J. B., Rajan J. A. Recent advancement in cooling technologies of solar photovoltaic (PV) system. *FME Transactions* 2018:46(4):575–584. https://doi.org/10.5937/fmet1804575S

[23] Mariam E., Ramasubramanian B., Reddy V. S., Dalapati G. K., Ghosh S., PA T. S., Chakrabortty S., Motapothula M. R., Kumar A., Ramakrishna S., Krishnamurthy S. Emerging trends in cooling technologies for photovoltaic systems. *Renewable and Sustainable Energy Reviews* 2024:192:114203. https://doi.org/10.1016/j.rser.2023.114203

[24] Choi S. M., Park C-D., Cho S-H., Lim B-J. Effects of wind loads on the solar panel array of a floating photovoltaic system – Experimental study and economic analysis. *Energy* 2022:256:124649. https://doi.org/10.1016/j.energy.2022.124649

[25] Demirdelen T., Alici H., Esenboğa B., Güldürek M. Performance and Economic Analysis of Designed Different Solar Tracking Systems for Mediterranean Climate. *Energies* 2023:16(10):4197. https://doi.org/10.3390/en16104197

[26] Sun L., Bai J., Pachauri R. K., Wang S. A horizontal single-axis tracking bracket with an adjustable tilt angle and its adaptive real-time tracking system for bifacial PV modules. *Renewable Energy* 2024:221:119762. https://doi.org/10.1016/j.renene.2023.119762

[27] Kolhe M. Techno-Economic Optimum Sizing of a Stand-Alone Solar Photovoltaic System. *IEEE Transactions on Energy Conversion* 2009:24(2):511–519. https://doi.org/10.1109/TEC.2008.2001455

[28] Kumar N. M., Vishnupriyan J., Sundaramoorthi P. Techno-economic optimization and real-time comparison of sun tracking photovoltaic system for rural healthcare building. *Journal of Renewable and Sustainable Energy* 2019:11(1):015301. https://doi.org/10.1063/1.5065366

[29] Ghabuzyan L., Pan K., Fatahi A., Kuo J., Baldus-Jeursen C. Thermal Effects on Photovoltaic Array Performance: Experimentation, Modeling, and Simulation. *Applied Sciences* 2021:11(4):1460. https://doi.org/10.3390/app11041460

[30] Glick A., Smith S. E., Ali N., Bossuyt J., Recktenwald G., Calaf M., Cal R. B. Influence of flow direction and turbulence intensity on heat transfer of utility-scale photovoltaic solar farms. *Solar Energy* 2020:207:173–182. https://doi.org/10.1016/j.solener.2020.05.061

[31] Lacombe F. Vérification et validation d'une loi de paroi consistante du modèle de turbulence K-w SST, 2017.

[32] Al-Bana A. S., Zahran S., Ahmed M. M., Al-Sayaad K. M. Performance Analysis and Validation of Different Meshing Techniques Used for Computational Fluid Dynamics Simulation. *2022 International Telecommunications Conference (ITC-Egypt)* 2022:1–5. https://doi.org/10.1109/ITC-Egypt55520.2022.9855763

[33] Heinrich R. Implementation and Usage of Structured Algorithms within an Unstructured CFD-Code. *New Results in Numerical and Experimental Fluid Mechanics V* 2006:430–437. https://doi.org/10.1007/978-3-540-33287-9_53

[34] Schlipf M., Tismer A., Riedelbauch S. On the application of hybrid meshes in hydraulic machinery CFD simulations. *IOP Conference Series: Earth and Environmental Science* 2016:49(6):062013. https://doi.org/10.1007/978-3-540-33287-9_53

[35] Kowarsch U., Hofmann T., Keßler M., Krämer E. Adding Hybrid Mesh Capability to a CFD-Solver for Helicopter Flows. *High Performance Computing in Science and Engineering ´16* 2016:461–471. https://doi.org/10.1007/978-3-319-47066-5_31

[36] NASA Prediction of Worldwide Energy Resources (POWER) Data Access Viewer [Online]. [Accessed 15.05.2025]. Available: https://power.larc.nasa.gov/data-access-viewer/

[37] Tominaga Y., Blocken B. Wind tunnel experiments on cross-ventilation flow of a generic building with contaminant dispersion in unsheltered and sheltered conditions. *Building and Environment* 2015:92:452–461. https://doi.org/10.1016/j.buildenv.2015.05.026